Computations of Turbulent Flow Beyond Backward-Facing Steps Using Reynolds-Stress Closure

R. S. Amano* and P. Goel†
University of Wisconsin, Milwaukee, Wisconsin

A numerical study is reported on the flow over a backward-facing step. The turbulence model employed is a hybrid model of Boussinesq viscosity and Reynolds-stress turbulence closure in which all of the terms are computed by using the Reynolds-stress closure except the diffusion terms of momentum, k, and ϵ equations. The computations are made for two different step ratios, $Y_0/H = 2$ and 3, and the results are compared with the k-ϵ model and an algebraic stress model, as well as the experimental data. As a consequence, it is concluded that the present model produces better results in the flow redeveloping region; however, the model still needs some modification for the computation in the recirculating regions.

Nomenclature

B_1, B_2, B_3 = constants used in turbulence model
C_1, C_2, C_D,
$C_{\epsilon 1}, C_{\epsilon 2}, C_\mu$ = coefficients used in turbulence model
D_{ij} = diffusion of $u_i u_j$
G = generation rate of turbulence kinetic energy, k
H = step height
k = turbulence kinetic energy
p = pressure fluctuation
P = mean pressure
P_{ij} = generation rate of Reynolds stresses
Q_{ij} = generation rate used in pressure-strain correlation
Re_θ = Reynolds number based on momentum thickness, θ
u = fluctuating velocity
U = mean velocity
x = Cartesian coordinate
x_r = length of reattachment
Y_0 = height of inlet flow section
z = coordinate normal to the wall
δ_{ij} = Kronecker delta
δA = area of numerical cell
ϵ = energy dissipation rate
ϵ_x = grid expansion factor in the x direction
μ = dynamic viscosity
μ_t = turbulent viscosity
ρ = density
$\sigma_k, \sigma_\epsilon$ = Prandtl numbers for k and ϵ
ϕ_{ij} = pressure-strain correlation

Subscripts

i,j,k,m = tensor notations
w = wall values

Introduction

FLOW in a channel with steps or sharp bends occurs in many engineering applications, such as airfoils with separation bubbles, combustors, heat exchangers, etc. While there have been significant contributions in this field, current understanding of the process is still relatively poor, partly because the flows in these geometries are complex, and partly because theoretical models developed to date are limited in predicting a wide range of parameters in separating, reattaching, and recirculating flows.

Bradshaw and Wong[1] and Smyth[2] measured turbulence quantities in the reattachment and redeveloping regions and reported that the center of the reattached shear layer still has most of the characteristics of a free shear layer as many as 50 step heights downstream of the reattachment point. This suggests that the large-scale eddies that develop in the separated free shear layer persist in the reattachment and redeveloping regions. However, the turbulent shear stress in the reattaching layer is much larger than the shear stress in an ordinary plane mixing layer and decreases rapidly near the reattachment point.

Eaton and Johnston[3] focused their measurements on the separated flow over a backward-facing step. A comparison with a plane mixing layer showed that the normal components of Reynolds stresses in the shear layer near the reattachment point were 10-20% higher than typical values measured in the plane mixing layers. However, the values of shear stress were of about the same order as those of plane mixing layers in most of the region upstream of the reattachment. It was also shown that the reattaching layer was similar to a plane mixing layer upstream of the reattachment region. These observations indicate that many parameters could be predicted in the reattaching shear layer by using simple mixing-layer data; and, consequently, the turbulence models used in a mixing-layer flow would still be adequate for the reattaching shear layer.

Theoretical studies on turbulence modeling for a wide range of flow patterns are available. Among the existing models, the so-called Reynolds-stress model (RSM) of turbulence, which provides transport equations for all of the Reynolds stresses, can provide individual stress behaviors while the viscosity-based models such as the k-ϵ model cannot. A model of this class was first proposed by Rotta,[4] and has been developed and improved by researchers.[5-8] The correlation of pressure strain was proposed by Naot et al.[6] and Launder et al.[8] Naot et al. evaluated the pressure-strain correlation term by integrating over space after inserting a conjectured form for the two-point correlation functions, whereas Launder et al.[8] obtained the results by assuming a fourth-order tensor consisting of linear Reynolds-stress elements. As a simplified Reynolds-stress closure model, an algebraic stress model that does not possess both convection and diffusion terms was developed in a similar manner by Rodi.[9]

Received May 9, 1984; revision received Oct. 11, 1984.

*Associate Professor, Department of Mechanical Engineering. Member AIAA.

†Graduate Student, Department of Mechanical Engineering.

In the authors' previous paper[10] several proposed closures for the Reynolds-stress model were tested for heat-transfer characteristics along pipe walls of axisymmetric sudden expansion cylinders. After computation using several different models, it was found that the pressure-strain correlation proposed by Launder et al.[8] showed slightly better agreement with experimental data for Nusselt number distributions along the pipe walls. Moreover, an incorporation of the wall correction terms in the pressure strain also improved predictions about 5-10%.

In this study, a refined part of the full Reynolds-stress closure is adapted and merged into the Boussinesq viscosity model for the computation of a turbulent flow over a backward-facing step. The results are compared with the experimental data of mean velocity profiles and Reynolds stresses in several different positions in the channel downstream of the step. The present model is also compared with the $k\sim\epsilon$ model and the algebraic stress model.

Mathematical Model

The steady, two-dimensional form of the continuity and momentum equations describing the flowfield is used in this study.

Continuity:

$$\frac{\partial}{\partial x_j}(\rho U_j)=0 \tag{1}$$

Momentum:

$$\frac{\partial}{\partial x_j}(\rho U_i U_j)=-\frac{\partial}{\partial x_i}+\frac{\partial}{\partial x_j}\left[\mu\left(\frac{\partial U_i}{\partial x_j}+\frac{\partial U_j}{\partial x_i}\right)-\rho\overline{u_i u_j}\right] \tag{2}$$

Closure of this momentum equation was achieved by relating the Reynolds stresses to the mean strain rate through the Boussinesq approximation

$$-\rho\overline{u_i u_j}=\mu_t\left(\frac{\partial U_i}{\partial x_j}+\frac{\partial U_j}{\partial x_i}\right)-\frac{2}{3}\delta_{ij}\rho k \tag{3}$$

where the turbulent viscosity is defined in terms of a characteristic velocity $k^{1/2}$ and a characteristic length $k^{3/2}/\epsilon$ as

$$\mu_t=C_\mu\rho k^2/\epsilon \tag{4}$$

The turbulence model used to determine the turbulent viscosity is the high Reynolds number form of the $k\sim\epsilon$ model given as

$$\frac{\partial}{\partial x_j}(\rho U_j k)=\rho(G-\epsilon)+\frac{\partial}{\partial x_j}\left[\left(\mu+\frac{\mu_t}{\sigma_k}\right)\frac{\partial k}{\partial x_j}\right] \tag{5}$$

$$\frac{\partial}{\partial x_j}(\rho U_j \epsilon)=\frac{\rho\epsilon}{k}(C_{\epsilon_1}G-C_{\epsilon_2}\epsilon)+\frac{\partial}{\partial x_j}\left[\left(\mu+\frac{\mu_t}{\sigma_\epsilon}\right)\frac{\partial \epsilon}{\partial x_j}\right] \tag{6}$$

where the generation rate of the turbulence kinetic energy can be expressed as

$$G=-\overline{u_i u_j}\frac{\partial U_i}{\partial x_j} \tag{7}$$

The values for the constants used above are: $C_\mu=0.09$, $C_{\epsilon 1}=1.44$, $C_{\epsilon 2}=1.92$, $\sigma_k=1.00$, and $\sigma_\epsilon=1.30$.

Although the closures of diffusive actions in the transport equations of the momentum, k and ϵ are made by using the Boussinesq viscosity approximation, the generation rate of turbulence [Eq. (7)] is evaluated in two ways: 1) by the Boussinesq approximation as shown in Eq. (3), and 2) by the model based on the Reynolds-stress closures. The latter set of equations is not a pure Reynolds-stress model but is a "modified" Reynolds-stress model (RSM), while the former is equivalent to the standard k-ϵ model.

The transport equations for the Reynolds stresses are

$$\frac{\partial}{\partial x_k}(U_k\overline{u_i u_j})=P_{ij}-\epsilon_{ij}+\phi_{ij}+\phi_{ij,w}+D_{ij} \tag{8}$$

where

$$P_{ij}=-\left(\overline{u_j u_k}\frac{\partial U_i}{\partial x_k}+\overline{u_i u_k}\frac{\partial U_j}{\partial x_k}\right)\text{: generation} \tag{9}$$

$$\epsilon_{ij}=2\nu\overline{\frac{\partial u_i}{\partial x_k}\frac{\partial u_j}{\partial x_k}}\text{: dissipation} \tag{10}$$

$$\phi_{ij}=\overline{\frac{p}{\rho}\left(\frac{\partial u_i}{\partial x_j}+\frac{\partial u_j}{\partial x_i}\right)}\text{: pressure-strain correlation} \tag{11}$$

and

$$D_{ij}=-\frac{\partial}{\partial x_k}(\overline{u_i u_j u_k})\text{: diffusion} \tag{12}$$

Equation (10) was approximated by the form given by Rotta.[4]

$$\epsilon_{ij}=\tfrac{2}{3}\delta_{ij}\epsilon \tag{13}$$

The pressure-strain term [Eq. (11)] was determined by combining Rotta's[4] linear return-to-isotropy hypothesis and the linear approximation of Launder et al.[8] The results are as follows:

$$\phi_{ij}=-C_1\epsilon\left(\frac{\overline{u_i u_j}}{k}-\frac{2}{3}\delta_{ij}\right)-B_1\left(P_{ij}-\frac{2}{3}\delta_{ij}G\right)$$
$$-B_2 k\left(\frac{\partial U_i}{\partial x_j}+\frac{\partial U_j}{\partial x_i}\right)-B_3\left(Q_{ij}-\frac{2}{3}\delta_{ij}G\right) \tag{14}$$

where

$$B_1=(C_2+8)/11,\quad B_2=(30C_2-2)/55$$
$$B_3=(8C_2-2)/11,\quad C_1=1.5,\quad C_2=0.4 \tag{15}$$

and

$$Q_{ij}=-\left(\overline{u_i u_k}\frac{\partial U_k}{\partial x_j}+\overline{u_j u_k}\frac{\partial U_k}{\partial x_i}\right) \tag{16}$$

The pressure-strain correlation with a near-wall correction is given as

$$\phi_{ij,w}=\left[0.125\frac{\epsilon}{k}\left(\overline{u_i u_j}-\frac{2}{3}k\delta_{ij}\right)+0.015(P_{ij}-Q_{ij})\right]\frac{k^{3/2}}{\epsilon z} \tag{17}$$

where z is a coordinate taken normal to the wall. Thus, if the point of interest is close to two plates (say, z_1 to one plate and z_2 to the other), then z is chosen to be

$$z=\min(z_1,z_2) \tag{18}$$

Finally, the diffusion rate [Eq. (12)] is evaluated as

$$D_{ij}=C_D\frac{\partial}{\partial x_k}\left(\frac{k}{\epsilon}\overline{u_k u_m}\frac{\partial\overline{u_i u_j}}{\partial x_m}\right) \tag{19}$$

where C_D is a constant with a value of 0.25 determined by a computer optimization.

It should be noted that both convection and diffusion rates of the Reynolds stresses are neglected in the so-called algebraic-stress model (ASM), whereas they are kept in the present RSM.

Numerical Method

The solution method of Eqs. (1-8) is the same finite volume method employed in the TEACH code,[11] while the differencing scheme is the modified hybrid scheme of Amano,[12] in which the combined mode of convection and diffusion is derived by expanding the analytical one-dimensional solution up to the fourth-order term. The cell structure for mean-velocity components is the staggered system in which the locations of the mean velocities U_1 and U_2 are shifted a half-cell in the x_1 and x_2 directions, respectively. All of the normal Reynolds stresses ($\overline{u_i^2}$) are evaluated at the scalar node point along with P, k, and ϵ. However, the shear Reynolds stress ($\overline{u_1 u_2}$) is located at the southwest corner of the scalar cell. This is because the main driving strains for the shear stress are $\partial U_1/\partial x_2$ and $\partial U_2/\partial x_1$, which can easily be evaluated without any interpolations.

Boundary Conditions

There are three different types of boundary conditions to be specified for the computation of a flow in the channel, as shown in Fig. 1: inlet, outlet, and wall boundary conditions.

At the inlet, all of the quantities are specified according to the fully developed condition. At the outlet, a continuative flow condition is applied where gradients of flow properties in the flow direction are zero (Neumann conditions), i.e., $\partial\phi/\partial x = 0$, where $\phi = U_i$, k, ϵ, $u_i u_j$, etc. This outlet is located about $120H$ downstream from the step so that its influence on the main flow region is negligibly small.

At the wall boundaries, however, the velocities and turbulence quantities must be specified functionally according to the drag law or the law of the wall. For example, the tangential velocity can be expressed in terms of wall shear stress as a functional expression of the boundary condition coupled with the no-slip condition as

$$F = \tau \delta A \tag{20}$$

where δA = wall area of the cell. The velocity component normal to the wall is simply set as zero. The wall boundary values for k and ϵ are determined by means of wall functions based on the assumption of a logarithmic near-wall velocity distribution that allows the wall shear stress to be extracted from the "log law" and the value of velocity parallel to the wall to be computed along the grid line closest to the wall. Near-wall effects on the turbulence structure associated with steep velocity variations are also taken into account by introducing appropriate modifications to the generation and dissipation of the turbulent energy and the energy dissipation rate for the finite volume adjacent to the wall.[12]

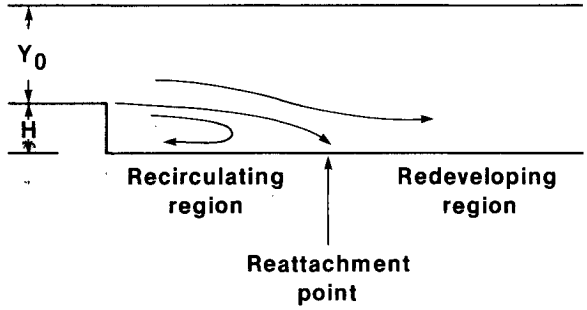

Fig. 1 Flow domain.

The boundary values for the Reynolds stresses are determined as

$$\overline{u_1^2} = 1.214k, \quad \overline{u_2^2} = 0.238k, \quad -\overline{u_1 u_2} = -0.238k + \frac{x_2}{\rho}\frac{dP}{dx_1} \tag{21}$$

in the wall-adjacent numerical cells. These boundary conditions are developed noting the following points: 1) the coefficients in the normal stresses represent a consensus of several reported wall flows, and 2) the boundary condition for the shear stress is given by the mean momentum equation. The details of the derivation of Eq. (21) are given in Ref. 16.

Computing Details

Exploratory tests were made for different mesh sizes to investigate an optimum grid-independent state. Figure 2 represents a length of reattachment for different grid expansion factors in the x direction ranging from 1.01 to 1.05 and for different numbers of grid points in the x and y directions. The larger value of the expansion factor ϵ_x creates a finer mesh in the recirculating region, while it results in a coarser mesh size in the downstream region far from the step. As shown, the variation in the length does not exceed 2% between the medium value of 1.03 and the relatively fine value of 1.05. Also, the grid system almost reaches a grid-independent state around 40 grid points for both the x and y directions. For all of the computations, a 42×42 grid system is used with an expansion factor of 1.03 in the x direction.

In the computation of the Reynolds-stress equations, initial stress values have to be specified properly so as not to cause numerical divergence, since the system of equations is rather unstable. This instability is mainly due to an explicit form of the Reynolds-stress equations which contain Reynolds stresses in all of the terms on the right-hand side except ϵ_{ij}. This problem was overcome by starting the computation with the $k \sim \epsilon$ model and then switching the model to the RSM after the flowfield became stabilized.[10] The computations were begun with the Boussinesq viscosity model of Eqs. (5) and (6). After about 400 iterations, the RSM was brought in, and the computations were continued until the maximum residual source of the mass flow rate or momentum reached 1.5%. Complete convergence was attained in 600-700 total iterations.

Discussion of Results

The flow in the channel in Fig. 1 was computed by using the models described in the preceding section, and the results were compared with available experimental data.

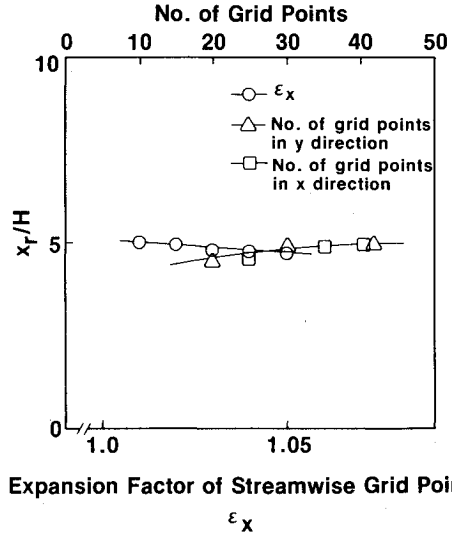

Fig. 2 Reattachment length for different grid size.

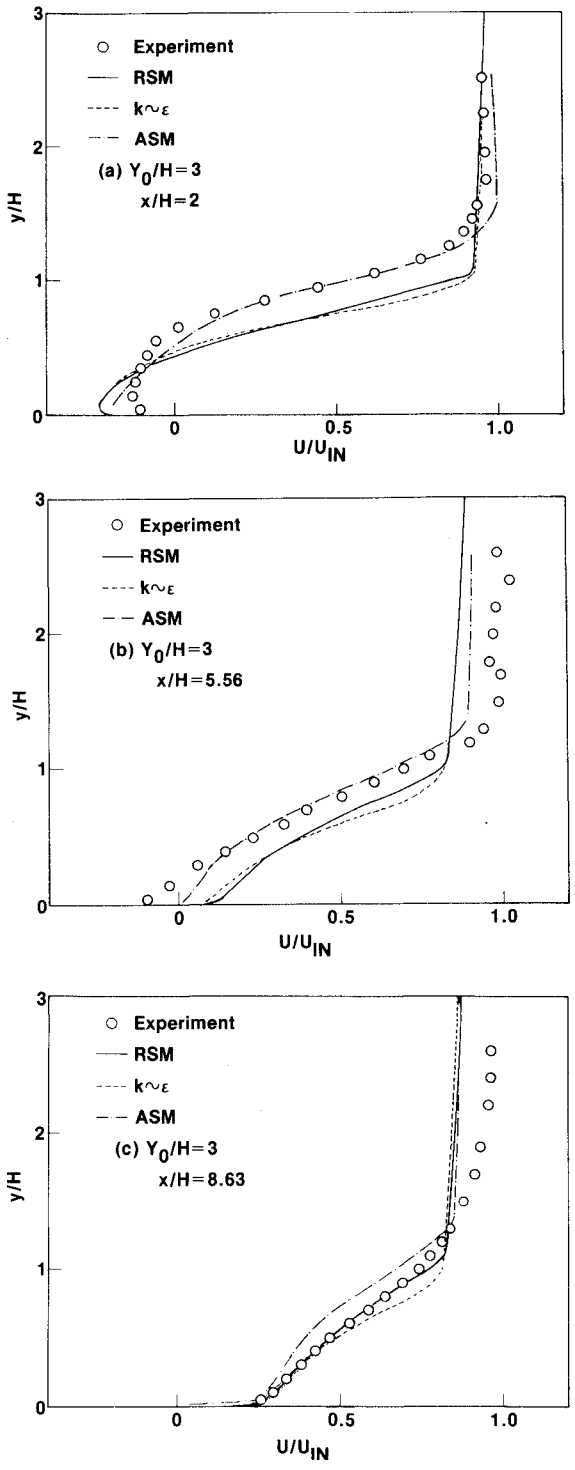

Fig. 3 Mean streamwise velocity profile.

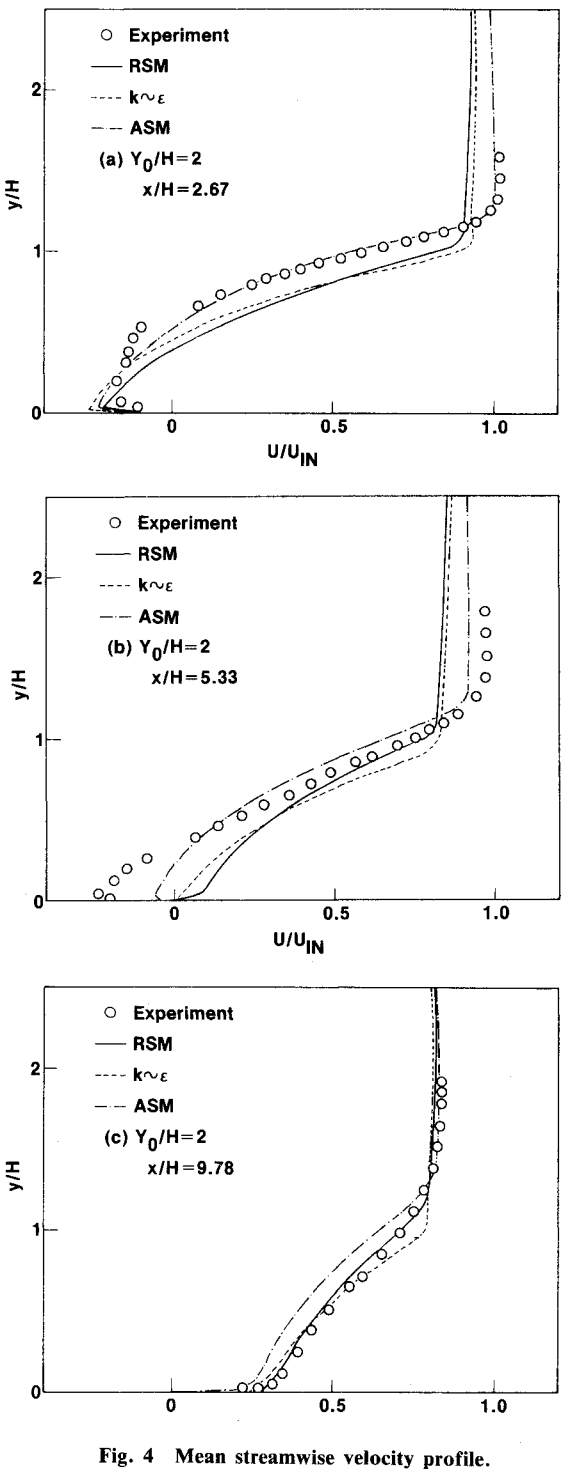

Fig. 4 Mean streamwise velocity profile.

Figure 3 shows the velocity profiles at several different locations along the flow stream for the channel step ratio $Y_0/H=3$ and $Re_\theta=5000$. Both of the computations by the $k\sim\epsilon$ model and RSM were compared with the experimental data of Seegmiller and Driver[13] at three streamwise positions: $x/H=2$, 5.56, and 8.63; where the reattachment point was about $x_r/H\simeq 5.0$. Thus, $x/H=2$ corresponds to the position in the recirculating region, $x/H=5.56$ to the position near the reattachment point, and $x/H=8.63$ is the position in the flow redeveloping region. Thus, it is observed that agreement between the experimental data and computational results in the recirculating and reattachment regions is not as good as in the redeveloping region. This is because the numerically predicted reattachment length, $x_r/H=5$, is somewhat different from that determined by the experiment, $x_r/H=7$. Moreover, although the difference between the computations by the $k\sim\epsilon$ and the RSM models is not remarkable, the RSM model consistently gives slightly better results.

Figure 4 shows the velocity profiles for the step ratio $Y_0/H=2$ in three locations: $x/H=2.67$, 5.33, and 9.78. The location $x/H=5.33$ is very near the reattachment point since the computed x_r/H is about 5.5. In addition, the computations are compared with the experimental data of Kim et al.,[14] where the trend of the prediction is quite similar to that in Fig. 3. However, in this case, the agreement between experiment and computation in the recirculating region is better than that found near the reattachment point. The

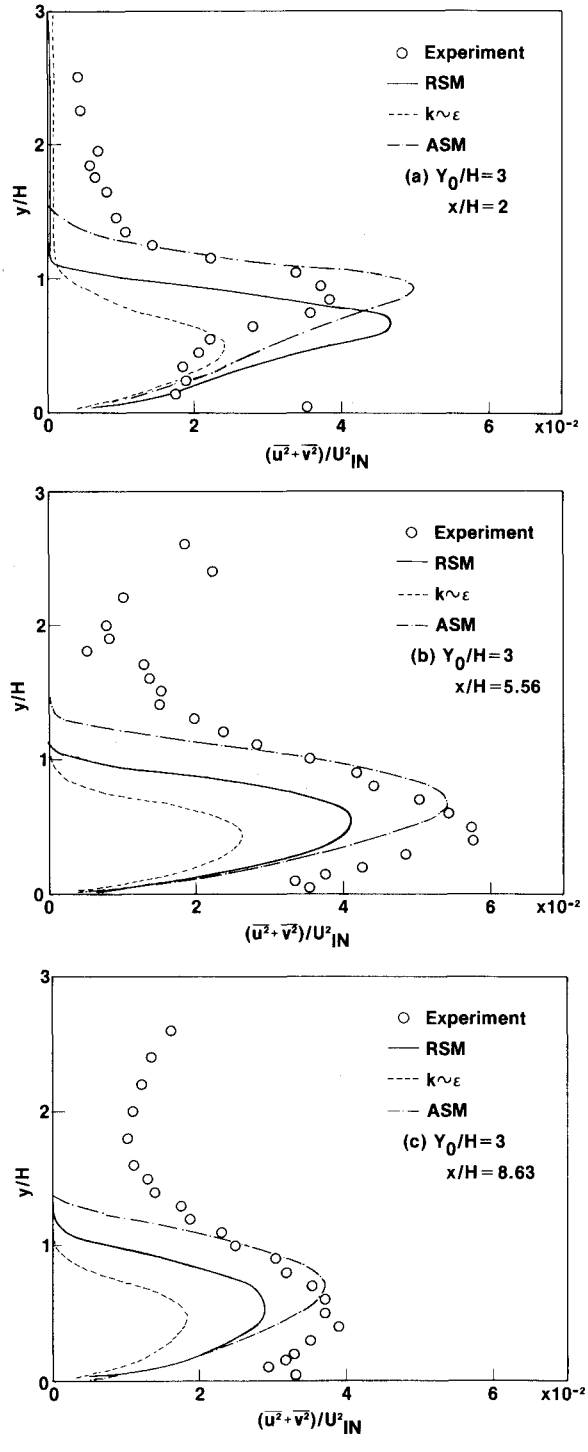

Fig. 5 Reynolds normal stress profile.

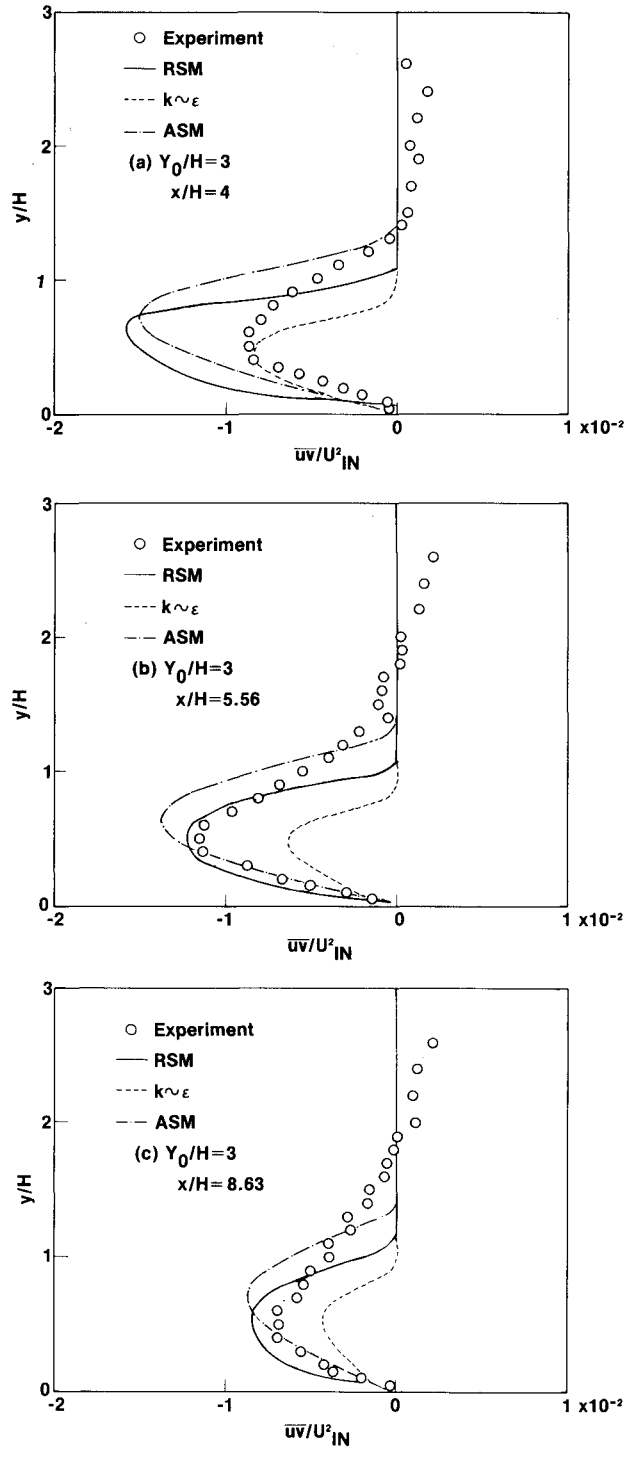

Fig. 6 Reynolds shear stress profile.

disagreement near the reattachment point is due to a discrepancy in the prediction of the reattachment length between the experiment ($x_r/H=7$) and the computation ($x_r/H=5.5$).

In Figs. 3 and 4, the computations by an algebraic stress model (ASM) made by Sindir[15] are also compared. The best agreement for the recirculating region is predicted by the ASM and for the redeveloping region by the RSM. It is also noted that the difference between the $k\sim\epsilon$ model and the RSM is larger in Fig. 4 than in Fig. 3.

As discussed, the proper turbulence model is dependent on the location within the flowfield. In the recirculating region, the RSM provides slightly better predictions near the wall. However, in the shear flow, the ASM gives the best agreement with experiment. In the reattachment region, the RSM shows the slowest velocity recovery performance while at the same time in the redeveloping region it shows the best prediction. Since the behavior of the mean velocity is closely related to the performance of Reynolds stresses, next we will examine the action of normal and shear stresses in the flow region across the streamwise flow.

Figures 5 and 6 show the normal and shear stress profiles, respectively, for the channel expansion of $Y_0/H=3$, which correspond to the velocity profiles in Fig. 3. The experimental data of Seegmiller and Driver[13] are also shown in these figures. The normal stresses increase rapidly with distance from the bottom wall and reach their maxima at about $y/H=1.0$ in the recirculating region and at $y/H=0.5$-0.7 in

the reattachment and redeveloping regions. The stresses then decrease to very small values at approximately $y/H = 1.3$-1.5. It is of interest that the y location of the peak moves upward in the order of the k-ϵ, RSM, and ASM models. The level of normal stresses also increases in the same order as the peak location. A similar trend is also observed for the shear stress distributions, except that they have negative values.

With regard to the comparison between measurements[13] and computations, the predictions by the ASM seem to be better for the normal stresses, while those by the RSM are closer to the experimental data for the shear stresses. The levels of the Reynolds stresses predicted by the k-ϵ model are always too low.

Observation of these Reynolds stresses indicates that the performance of the Reynolds-stress prediction does not necessarily accord with the computation of the mean velocity profiles shown in Fig. 3. At $x/H = 2$, the RSM gives better agreement but the ASM is superior for normal stresses in the redeveloping region. Generally, we see the success of the Reynolds-stress closure in the prediction of the shear stress distributions.

Conclusions

In this study, a hybrid model of the Boussinesq viscosity and a full Reynolds-stress closure model was developed. The flow computations of two different step ratios are demonstrated and the results are compared with the experimental data, k-ϵ, and algebraic stress models. As a result, the following conclusions emerge:

1) The relative performance of the models is strongly dependent on the flow region. Hence, the best prediction of the flowfield is not necessarily obtained by the same model in recirculating, reattaching, and redeveloping regions.

2) The Reynolds-stress closure model predicts the mean velocity profiles best in the redeveloping region, but not in the recirculating and reattachment regions; the algebraic-stress model shows better results in the latter regions.

3) All of the models tested herein underpredict the reattachment length despite the limited improvements with the RSM.

References

[1]Bradshaw, P. and Wong, F.Y.F., "The Reattachment and Relaxation of a Turbulent Shear Layer," *Journal of Fluid Mechanics*, Vol. 52, Pt. 1, 1972, pp. 113-135.

[2]Smyth, R., "Turbulent Flow Over a Plane Symmetric Sudden Expansion," *Journal of Fluids Engineering*, Vol. 101, No. 3, 1979, pp. 348-353.

[3]Eaton, J. K. and Johnston, J. P., "A Review of Research on Subsonic Turbulent Flow Reattachment," *AIAA Journal*, Vol. 19, Sept. 1981, pp. 1093-1100.

[4]Rotta, J. C., "Statistische Theorie Nichthomogener Turbulenz," *Zeitschrift für Physik*, Vol. 129, 1951, pp. 547-572.

[5]Daly, B. J. and Harlow, F. H., "Transport Equations of Turbulence," *The Physics of Fluids*, Vol. 13, No. 11, 1970, pp. 2634-2649.

[6]Naot, D., Shavit, A., and Wolfshtein, M., "Two-Point Correlation Model and the Redistribution of Reynolds Stress," *The Physics of Fluids*, Vol. 16, June 1973, pp. 738-743.

[7]Lumley, J. L. and Khajeh Nouri, B., "Computational Modeling of Turbulent Transport," *Advances in Geophysics*, Vol. 18A, 1974, pp. 169-192.

[8]Launder, B. E., Reece, G. J., and Rodi, W., "Progress in the Development of a Reynolds-Stress Turbulence Closure," *Journal of Fluid Mechanics*, Vol. 68, 1975, pp. 537-566.

[9]Rodi, W., "The Prediction of Free Boundary Layers by Use of a Two-Equation Model of Turbulence," Ph.D. Thesis, University of London, U.K., Dec. 1972.

[10]Amano, R. S. and Goel, P., "A Numerical Study of a Separating and Reattaching Flow by Using Reynolds-Stress Turbulence Closure," *Numerical Heat Transfer*, Vol. 7, No. 3, 1984, pp. 343-357.

[11]Gosman, A. D. and Ideriah, F.J.K., "TEACH-T: A General Computer Program for Two-Dimensional, Turbulent, Recirculating Flows," Mechanical Engineering Dept., Imperial College, London, Rept., June 1976.

[12]Amano, R. S., "Development of Turbulent Near-Wall Model and Its Application to Separated and Reattached Flows," *Numerical Heat Transfer*, Vol. 7, No. 1, 1984, pp. 59-75.

[13]Seegmiller, H. L. and Driver, D. M., Private communications, 1984.

[14]Kim, J., Kline, S. J., and Johnston, J. P., "Investigation of Separation and Reattachment of a Turbulent Shear Layer: Flow Over a Backward Facing Step," Thermosciences Div., Dept. of Mechanical Engineering, Stanford University, Stanford, Calif., Rept. MD-37, 1978.

[15]Sindir, M. M., "Effects of Expansion Ratio on the Calculation of Parallel-Walled Backward-Facing Step Flows: Comparison of Four Models of Turbulence," ASME Paper 83-FE-10, 1983.

[16]Amano, R. S. and Goel, P., "A Study of Reynolds-Stress Closure Model," NASA-CR-174242, 1985.